EUROPEAN ORGANIZATION FOR NUCLEAR RESEARCH

Proposal to the ISOLDE and Neutron Time-of-Flight Committee

Following HIE-ISOLDE Letter of Intent I-097 and I-099

Single-Particle Structure in Neutron-Rich Calcium Isotopes

October 2012

S.J. Freeman[1], A. Andreyev[2], S. Bönig[10], P.A. Butler[4], M.P. Carpenter[5], W.N. Catford[6], J. Cederkall[7], R. Chapman[2], T.E. Cocolios[1], F. Flavigny[8], L. Gaffney[4], D. Di Julio[7], C.R. Hoffman[5], M. Huyse[8], S. Ilieva[10], R.V.F. Janssens[4], D. Jenkins[9], B.P. Kay[5], T.Kröll[10], D. Mücher[3], N. Nowak[3], G. O'Neill[4], R. Orlandi [8], R. Raabe[8], M. Scheck[10], J.P.Schiffer[5], J.S. Thomas[1], P. Van Duppen[8], R. Wadsworth[9], N. Warr[11], and S. Zhu[5].

[1] University of Manchester, UK; [2] University of the West of Scotland, UK; [3]Technischen Universität München, Germany; [4]University of Liverpool, UK; [5]Argonne National Laboratory, USA [6] University of Surrey, UK; [7] Lund University, Sweden, [8]KU Leuven, Belgium, [9]University of York, UK; [10]Technischen Universität Darmstadt, Germany; and [11] Universität zu Köln, Germany.

Spokesperson: sean.freeman@manchester.ac.uk

Contact person: Magdalena Kowalska

CERN-INTC-2012-057 / INTC-P-358
09/10/2012

Abstract

It is proposed to study the $d(^{50}\mathrm{Ca},p)$ reaction using 5 MeV/u beams from HIE-ISOLDE. The deduced single-particle strengths will be used to benchmark calculations for the neutron-rich *fp* shell which differ in their predictions of single-particle spacing around *N=34.* Outgoing light-ions will be momentum analysed using a new solenoidal spectrometer.

Requested shifts: [13] shifts
Beamline: [2nd beamline: solenoidal spectrometer]

1. Introduction

One of the motivations for studying very exotic nuclei is the expectation that macroscopic alterations induced by weak binding will affect the microscopic structure of the nucleus. Motivated by these expectations, recent advances have revealed a surprising evolution in single-particle structure, even in near-stable and moderately exotic systems where the weak-binding effects are unlikely to be significant. In lighter nuclei, changes are sufficient to destroy magic numbers seen near stability. Drifts in single-particle states also open up new gaps in single-particle levels and create new regions of relative stability. Similar trends in single-particle states have been observed in near-stable heavy nuclei, suggesting a ubiquitous phenomenon. Such changes have begun to be interpreted as the effects of the *N-N* interaction between protons and neutrons [1]. The gradual filling of particular orbits with one type of nucleon has an increasing interaction with orbitals containing the other type, driving an evolution in effective single-particle energies with nucleon number. The consequences of such evolution go beyond the quantum levels: single-particle structure influences other nuclear properties, including nuclear shapes and the modes of collective behaviour that are energetically favourable to the system.

2. Physics case

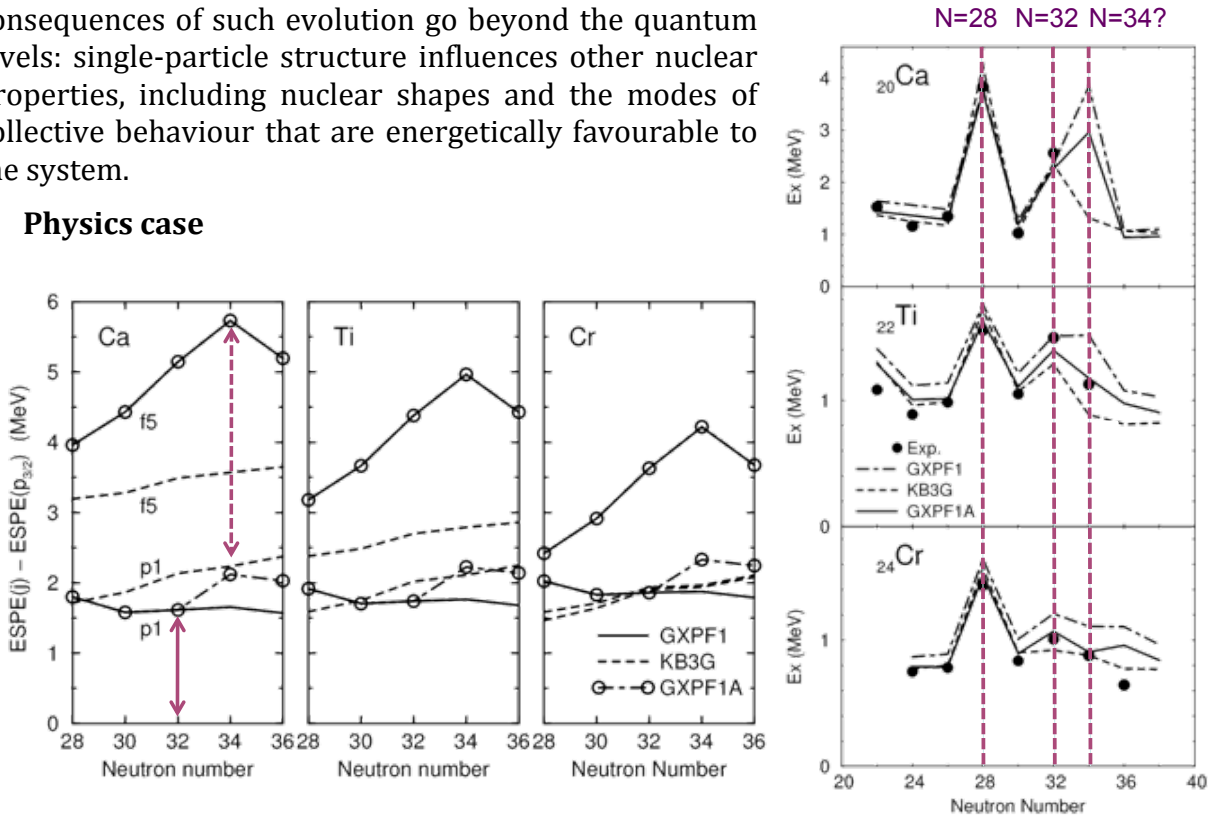

Figure 1: *(Left) Effective single-particle energies from calculations with three different shell-model interactions for Ca, Ti and Cr isotopes beyond N=28. The N=32 and the potential N=34 gaps in Ca are indicated. (RIGHT) Experimental first 2^+ energies compared to shell-model calculations. Figures from [2].*

Calcium isotopes lie at the beginning of the $f_{5/2}$ *p* shell where several novel shell closures have been observed and predicted. For example, a strong *N=32* sub-shell gap was proposed to explain the surprisingly large excitation energy of the first 2^+ state in ^{52}Ca compared to the corresponding state in ^{50}Ca (see discussion in [3] and references therein). Studies in neutron-rich titanium and chromium isotopes [4] have also seen a rise in the energy of the 2^+ state at *N=32*, although the effect is diminished with increasing atomic number. This gap is thought to arise from a large neutron $p_{3/2}$—$p_{1/2}$ separation, but the shell effect gradually dies in higher *Z* nuclei; the neutron $f_{5/2}$ is pushed down by interactions with increasing

numbers of $f_{7/2}$ protons closing the gap at *N=32*. Full *fp* shell-model calculations have become possible over the past decade and new effective interactions have been developed. These are able to accurately reproduce the systematics of the *N=32* gap in Ca, Ti and Cr isotopes (Ref. [2] and shown in Fig. 1). In calcium isotopes, a large separation between neutron $f_{5/2}$ and $p_{1/2}$ levels producing a sizeable *N=34* gap sometimes appears. This gap is somewhat controversial; it arises with the use of some particular effective interactions, but not others. This is due to different predicted single-particle evolution beyond ^{48}Ca, despite similar predictions for less exotic species. Predictions using the GXPF1A interaction show that in ^{49}Ca the neutron $p_{1/2}$ orbit is lower in energy compared to the $f_{5/2}$ state by 1.8 MeV [2] and other interactions give similar results. A difference arises as more neutrons are added; in GXPF1A calculations the gap between these orbitals increases significantly towards *N=34*, while using the KB3G interaction, for example, it is roughly constant. The difference appears to be due to differences in the *T=1* monopole effect [2].

The phenomenological approaches within the shell model have been very recently supplemented by microscopic calculations. Coupled-cluster methods using interactions from chiral effective field theory, have highlighted the need for three-body forces to reproduce the *N=32* shell closure [3]. Such calculations reproduce well the ground state and first excited states in the even *A<54* isotopes. The subshell closure at *N=34* still persists in the calculations, but is weaker than the GXPF1A predictions [3, 4].

Discrimination between predictions would clearly benefit from a measurement of the energy of the first 2^+ state in ^{54}Ca, but such experiments are currently very difficult. However, measurements of the $f_{5/2}$ and $p_{1/2}$ single-particle strengths in neutron-rich calcium isotopes would be a direct way of testing the shell-model calculations, and give an early indication of the validity of the predictions of the *N=34* gap.

Shell-model calculations within the neutron-rich *fp*-shell beyond *N=28* have been tested mainly against measured level energies and spins. Excited states have been populated in a variety of methods including β decay of fragmentation products; multinucleon transfer reactions; and charged-particle evaporation following the fusion of neutron-rich heavy ions. None of these methods have direct sensitivity to the underlying single-particle nature of the states populated. For example, an unambiguous statement concerning the presence of the *N=34* gap in ^{54}Ca has been difficult to reach from studies of γ rays from states in ^{52}Ca populated using deep-inelastic collisions [5, 7]. Such methods also exhibit selectivity (for example, a preference for yrast levels) that can limit their usefulness in populating single-particle strength. There are only a few studies that have gone beyond levels and spins by the measurement of B(E2) values [8] and by the use of knockout reactions [9]. Only near stability are traditional single-neutron transfer data available giving direct measurement of the single-particle contribution to the populated states (for example, in ^{49}Ca [10]).

As a first step, we propose to study the $d(^{50}\text{Ca},p)$ reaction to probe the single-particle nature of the ground and low-lying states of ^{51}Ca in a test of the shell-model predictions. Even though this system is fairly close to *N=28,* energetic trends of the effective single-particle energies predicted by different shell-model calculations already vary (Figure 1) and this should be related to differences in the single-particle content of the low-lying states, accessible through spectroscopic factors deduced from the experiment.

3. Methodology:

The mechanism of direct single-nucleon transfer is well established and the method can be used with some confidence to extract spectroscopic information. Identification of the

quantum numbers of the states populated can be performed on the basis of angular-distribution measurements. Spectroscopic factors, whilst not being observables in the strictest sense, can be extracted from measured cross sections to give a measure of the single-particle content of final states. Such analyses are to some extent model-dependent, but this is relatively well understood and the relative values of the spectroscopic factors are reasonably robust, as long as consistent analyses are performed. Recent studies have demonstrated that spectroscopic factors deduced within a systematic analysis procedure yield self-consistent results [11].

The availability of HIE-ISOLDE beams at 5.5 MeV/u mitigates worries concerning the contributions of non-direct reaction mechanisms to the *(d,p)* reaction at lower bombarding energies. The angular distributions at 5.5 MeV/u are characteristic of the ℓ transfers as shown in Figure 2.

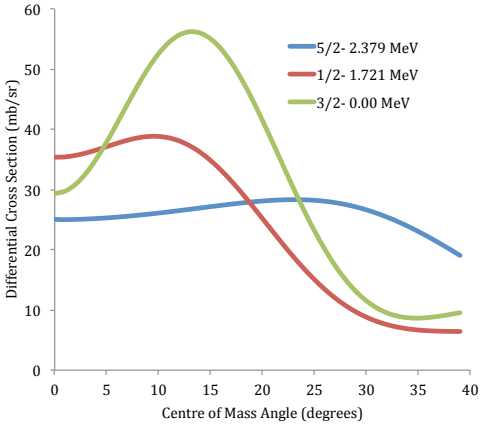

Figure 2: *DWBA predictions for the three most strongly populated states in the d(^{50}Ca,p) reaction at 5.5 MeV/u. Calculations here are for the full spectroscopic strength associated with the corresponding orbitals.*

4. Beam requirements:

In general, the minimum useful beam intensity is ~10^4 pps on target for transfer experiment of the order of 7-10 days. Beam purity is an important issue as ^{50}Ti is a likely contaminant. Measurements of the Z of ions recoiling from these transfer reactions are rather difficult due to the kinematics of the reaction and detector rate limitations. However, recent developments of laser ion sources have improved the purity of calcium ion beams at ISOLDE. In addition, the experimental setup will be able to tolerate ^{50}Ti contamination with similar intensity to the ^{50}Ca beam (see below). Recent measurements of the intensity of ^{51}Ca with UC480 at the HRS of 4x10^4 pps, suggest that intensities of ^{50}Ca are likely to be several 10^5 pps with the strong expectation of >10^4 pps of accelerated beam. These yields are in line with SC yields quoted in the ISOLDE database.

5. Equipment:

The experiment will use a solenoidal spectrometer [12] for momentum analysis of the outgoing protons from the reaction, similar to that in use at Argonne National Laboratory [13]. This design of spectrometer has several advantages compared to conventional charged-particle spectroscopy using silicon detectors for this proposal, beyond the much simpler and less complex detector system.

Firstly, it provides better proton energy resolution, where this is not limited by target energy-loss effects. This arises since the centre-of-mass energy is a simple linear function of the measured position and lab energy measured for protons at the axis of the solenoid, so the resolution is not limited by kinematic shift. Essentially, the lab energy resolution is identical to the CM energy resolution. Secondly, this linear relationship also means that the dispersion of different excited states in the ion-energy and Q-value spectra are the same. In the conventional approach, using Si at fixed angles, the non-linear relationship between proton energy and angle means that proton energy resolution is limited by kinematic shift

over the entrance angle. And when moving from a lab ion-energy spectrum to excitation energy, peaks become compressed together by factors of up to three, degrading the effective Q-value resolution. Even where target energy-loss effects compound the ion-energy resolution, the resulting Q-value spectrum with a solenoid still benefits from this lack of compression. As an example, a recent $d(^{86}\mathrm{Kr},p)$ measurement achieved an excitation energy resolution of ~70 keV [14].

Some conventional approaches use γ-ray measurements to recover resolution. This introduces an additional efficiency of ~10% due to the coincidence requirement, which can be compensated by using a thicker target but this compromises the particle resolution further. Measurements of the yield are complicated by the need for good γ-ray branching ratios and absolute efficiencies. A solenoidal system allows sufficient resolution from the measurement of outgoing ions alone. With regards to the current proposal, conventional methods of charged-particle spectroscopy are difficult since measurements are needed with good resolution (<70 keV) to allow separation from a peak due to the expected beam contaminant (see next section). The transfer to the ground state is important here; something that obviously cannot be done γ rays, but is also difficult to obtain with good resolution in conventional Si arrays.

6. Experimental Considerations:

The expected performance of the solenoid with the two beams ^{50}Ti/Ca is shown in Figure 3, where the proton energy is plotted as a function of position along the axis; different loci in this plot correspond to excited states. In real data these would be spread by the position (<1 mm) and proton energy (<70 keV) resolutions. A transformation is then applied to remove position dependence and project the final Q-value spectrum. The two sets of excited states corresponding to ^{50}Ti and ^{51}Ca are offset by the difference in Q-value.

The ^{50}Ti(d,p) reaction was performed many years ago and spectroscopic factors are available in the literature [15]. The known distribution of spectroscopic strength for ^{51}Ti is shown in Figure 3. Also shown is the distribution of spectroscopic strength for ^{51}Ca predicted by a shell-model calculation using the GXPF1A effective interaction [16]. Experimental energies of states below the neutron-separation energy in ^{51}Ca have been determined by γ-ray measurements following deep inelastic reactions [6], although spin-parities are only tentatively known. Given that the level densities of states populated is fairly low, with sufficient resolution the determination of peak yields should be relatively uncomplicated, as long as the contaminating beam intensity is of the same order of magnitude as ^{50}Ca. For example, the ground state of ^{51}Ca is close to a strong state in ^{51}Ti, but the separation is 126 keV, which should be easily resolved. The first excited ½$^-$ state will have a partially resolved shoulder, but should be disentangled with peak fitting.

In order to extract absolute cross sections, the product of the beam intensity and the areal density of deuterons in the target will be measured throughout the experiment. An annular Si surface-barrier detector positioned downstream from the target such that elastically scattered deuterons are intercepted and the luminosity deduced from the yield.

7. Beam Time Request:

In estimations of the rates, a CD_2 target of thickness 100μgcm^{-2}, a beam current of 10^4 pps, and a central axis silicon array with physical length that corresponds to the coverage of centre-of-mass angles from 5 to 30° have been assumed. Azimthuial coverage is taken to

be 75% and with *z* coverage of 70%. DWBA calculations are used for the cross sections, with a normalisation factor of 0.55 [11], integrated over the solid angle of the array.

Under these conditions, a state with 10% of the full spectroscopic strength is expected to be populated with a rate of 100 counts per shift. Given the arrray is envisaged to have ten pads which would each contribute one point in an angular distribution, 10 shifts of data collection would be needed to obtain good angular distributions for states with spectroscopic factors down to $C^2S=0.1$. Three shifts are requested to set up the system with the radioactive beam.

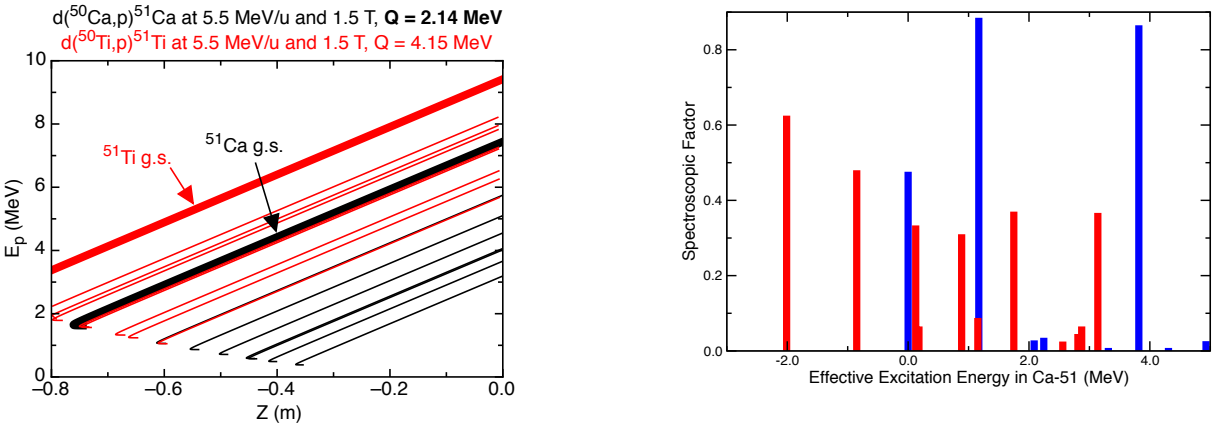

Figure 3: *(LEFT) Kinematic calculations for the d(^{50}Ca,p) reaction at 5.5 MeV/u, showing proton energies as a function of position along the solenoid axis. The loci corresponding to different states in ^{51}Ca are shown (black), with those for reactions with the excepted contaminant beam ^{50}Ti. (RIGHT) The expected (d,p) strength distributions for ^{51}Ca (blue), from a GXPF1A calculation [15], and for ^{51}Ti (red), using previously measured data (red), plotted against the effective excitation energy in ^{51}Ca. The width of the bars is equal to the upper limit for the expected the energy resolution (70 keV).*

8. References:

[1] For example, T. Otsuka et al., PRL 95, 232502 (2005).

[2] M. Honma et al. PRC 65, 061301 (2002) and Eur.Phys.J. A25, s01, 499 (2005).

[3] G. Hagen et al., PRL 109, 032502 (2102).

[4] Jason D Holt et al., JPHYSG 39, 85111 (2012).

[5] B. Fornal et al., PRC 77, 014304 (2008).

[6] J. I. Prisciandaro et al., PLB 510, 17 (2001) ; R. V. F. Janssens et al., PLB 546, 55 (2002).

[7] M. Rejmund et al., PRC 76, 021304 (2007).

[8] D.-C. Dinca et al., PRC 71, 041302(R) (2005) ; A. Burger PLB 622, 29 (2005).

[9] A. Gade et al., PRC 74, 021302 (2006).

[10] Y. Uozumi et al., NPA 576, 123 (1994).

[11] J.P. Schiffer et al., PRL 108, 022501 (2012).

[12] S.J. Freeman et al., INTC LOI INTC-I-099 (2010)

[13] J. Lighthall et al., NIMS A622, 97 (2010) ; Wuosmaa et al., NIMS A580, 1290 (2007).

[14] D.K. Sharp et al., J. Phys.: Conf. Ser.381, 012099 (2012) and submitted to PRC (2012).

[15] NDS 107, 2131 (2006); P. Wilhjelm et al. PR 166, 1121 (1968).

[16] M. Honma, Private Communication.

Appendix

DESCRIPTION OF THE PROPOSED EXPERIMENT

The experimental setup comprises: *Solenoidal spectrometer.*

Part of the Choose an item.	Availability	Design and manufacturing
Solenoidal spectrometer	☐ Existing	☐ To be used without any modification ☐ To be modified
	☒ New	☐ Standard equipment supplied by a manufacturer ☒ CERN/collaboration responsible for the design and/or manufacturing

HAZARDS GENERATED BY THE EXPERIMENT

Additional hazards:

Hazards	*Solenoidal Spectrometer*	*[Part 2 of the experiment/equipment]*	*[Part 3 of the experiment/equipment]*
Thermodynamic and fluidic			
Pressure	[		
Vacuum			
Temperature	4 [K]		
Heat transfer			
Thermal properties of materials			
Cryogenic fluid	Liquid helium, [atmospheric][Bar], ~2000[l]		
Electrical and electromagnetic			
Electricity	0 [V], 300 [A]		
Static electricity			
Magnetic field	<3.0 [T]		
Batteries	☐		
Capacitors	☐		
Ionizing radiation			
Target material	CD2		
Beam particle type (e, p, ions, etc)	50Ca		
Beam intensity	>1e04 pps		
Beam energy	5.5 MeV/u		
Cooling liquids			
Gases			
Calibration sources:	☐		
• Open source	☒		
• Sealed source	☐ [ISO standard]		
• Isotope			
• Activity			
Use of activated material:			
• Description	☐		

• Dose rate on contact and in 10 cm distance	[mSV]		
• Isotope			
• Activity			
Non-ionizing radiation			
Laser			
UV light			
Microwaves (300MHz-30 GHz)			
Radiofrequency (1-300MHz)			
Chemical			
Toxic			
Harmful			
CMR (carcinogens, mutagens and substances toxic to reproduction)			
Corrosive			
Irritant			
Flammable			
Oxidizing			
Explosiveness			
Asphyxiant	Helium		
Dangerous for the environment			
Mechanical			
Physical impact or mechanical energy (moving parts)			
Mechanical properties (Sharp, rough, slippery)			
Vibration			
Vehicles and Means of Transport			
Noise			
Frequency			
Intensity			
Physical			
Confined spaces	Vacuum Chamber		
High workplaces			
Access to high workplaces			
Obstructions in passageways			
Manual handling			
Poor ergonomics			

0.1 Hazard identification

3.2 Average electrical power requirements (excluding fixed ISOLDE-installation mentioned above): *(make a rough estimate of the total power consumption of the additional equipment used in the experiment)*

5 kW